Hippocampal storage and recall of neocortical 'What' - 'Where' representations Supplementary Material

Hippocampus (2024) doi: 10.1002/hipo.23636

August 23, 2024

Edmund T. Rolls
Oxford Centre for Computational Neuroscience, Oxford, UK
and University of Warwick, Department of Computer Science, Coventry CV4 7AL, UK
and Institute of Science and Technology for Brain Inspired Intelligence, Fudan University, Shanghai 200403, China
and

Chenfei Zhang
Institute of Science and Technology for Brain Inspired Intelligence, Fudan University, Shanghai 200403, China
and

Jianfeng Feng
University of Warwick, Department of Computer Science, Coventry CV4 7AL, UK
and Institute of Science and Technology for Brain Inspired Intelligence, Fudan University, Shanghai 200403, China

Corresponding author: Professor Edmund T. Rolls, Oxford Centre for Computational Neuroscience, Oxford, UK. Email: Edmund.Rolls@oxcns.org, Url: https://www.oxcns.org

1 Rate simulation of the hippocampal system

A description of the architecture that is simulated is shown in Fig. 1. The main text of the paper describes each stage of the circuitry. In this part of the Supplementary Material the Equations for the rate simulation are provided, and further background information is provided elsewhere (Rolls 1995). The convention is that the modules are named for example as EntoWhat (with the abbreviations shown in Fig. 1), and connections to NcWhat from EntoWhat are described as NcWhatFromEntoWhat.

1.1 Rate model: neocortex

During training, the random binary 0-1 patterns applied to NcWhat and NcWhere are passed to EntoWhat and EntoWhere to provide their inputs. Also during training, the backprojections from the EntoWhat and EntoWhere to NcWhat and NcWhere are modified by Hebbian associative learning as shown in Eq. 1 to allow later recall when the backprojections are active:

$$\delta w_{ij} = \alpha y_i x_j \tag{1}$$

where δw_{ij} is the change of the synaptic weight w_{ij} that results from the simultaneous (or conjunctive) presence of presynaptic firing x_j from the entorhinal cortex and postsynaptic firing of the neocortical neurons y_i, and α is a learning rate constant that specifies how much the synapses alter on any one pairing. One pairing is sufficient for each pattern pair, and the learning rate can be 1.

During recall, the backprojections to NcWhat and NcWhere from EntoWhat and EntoWhere operate by standard pattern association recall (Rolls 2023). The total activation h_i of a neocortical neuron i is the sum of all the activations produced through each strengthened synapse w_{ij} on the neocortical neuron by each active entorhinal neuron x_j. We can express this as

$$h_i = \sum_{j=1}^{C} x_j w_{ij} \tag{2}$$

where $\sum_{j=1}^{C}$ indicates that the sum is over the C input axons (or connections) indexed by j to each neuron. The activation h_i is converted into firing y_i. This conversion can be expressed as

$$y_i = \mathrm{f}(h_i) \tag{3}$$

where the function f is the activation function (Rolls 2023), which for this research was threshold binary (meaning that above a threshold of activation,

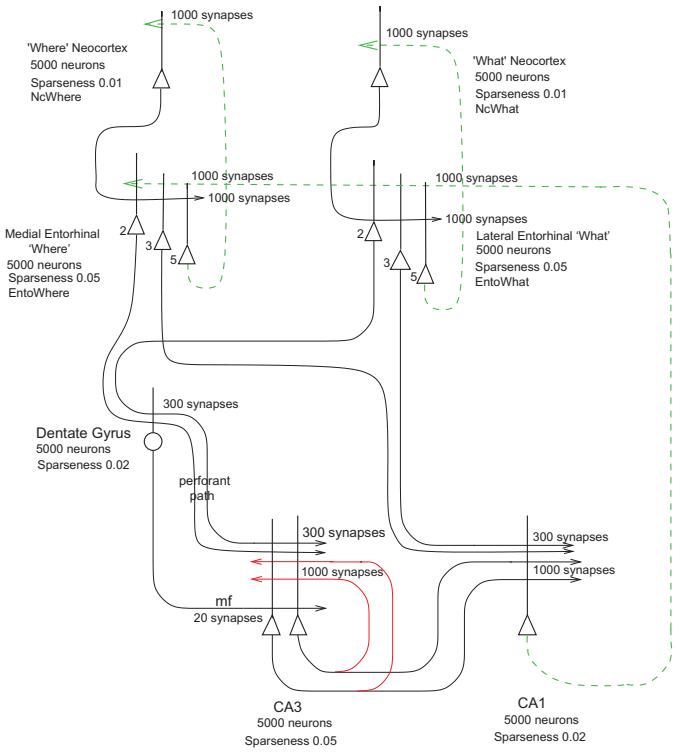

Figure 1: Simulation of neocortical 'What' and 'Where' inputs to the hippocampus for the storage of episodic memory, and for the recall of 'What' (object) and 'Where' (spatial view in primates or place in rodents) information back to the 'What' and 'Where' neocortex. The pyramidal cell bodies are shown as triangles, the dendrites as the thick lines above the cell bodies, and the axons as thin lines terminated with an arrow. The numbers of synapses shown are the numbers on any one neuron. The backprojection pathways for memory recall are shown in dashed green lines, and in red the CA3 recurrent collaterals via which 'What' and 'Where' representations present at the same time can be associated during episodic memory storage, and via which completion of a whole memory from a part can occur during recall. All synapses are associatively modifiable except for the Dentate Gyrus (DG) mossy fibre (mf) synapses on the CA3 pyramidal cells. The dentate granule cells, the CA1 cells, and the entorhinal cortex inputs from the neocortex operate as competitive networks. The CA3 cells operate as an autoassociation attractor network to implement completion. The backprojection connections shown in green operate as pattern association networks (Rolls 2023). The sparseness can be measured by the proportion of neurons with high firing rates (see text). The abbreviations used in this Supplementary Material for some of the modules are shown in this figure.

the firing rate was 1, and below the threshold it was 0). (A threshold linear activation function was also tested, with which if above the threshold, the firing was set to the activation.) The threshold was set to a value to produce the value for the sparseness shown in Fig. 1, where sparseness is defined for binary neurons as the proportion of the neurons with a high firing rate (Rolls 2023).

1.2 Rate model: entorhinal cortex

During training, the entorhinal cortex modules each act as a competitive network, which can be useful in categorisation (Rolls 2023). The firing rates of the entorhinal cortex neurons produced by the forward inputs from the neocortex are produced as described above for the neocortex with Eqs. 2 and 3. Then the synapses between the active inputs from the neocortex and the high firing rate entorhinal cortex neurons are associatively modified by the Hebb associative learning rule Eq. 1. Because all firing rates are positive, the synaptic weights are positive. In the competitive network, the length of the synaptic weight vector on each neuron is then normalized to a length of 1, so that the different neurons compete on an equal basis (Rolls 2023). Also during training, the backprojections from CA1 to EntoWhat and EntoWhere are modified by Hebbian associative learning as shown in Eq. 1 to allow later recall when the backprojections are active.

During recall, the backprojections to EntoWhat and EntoWhere from CA1 operate by standard pattern association recall (Rolls 2023) in a similar way to that described in Section 1.1 and Eqs. 2 and 3.

1.3 Rate model: CA1

During training, the CA1 acts as a competitive network, which is useful in categorising the necessarily separate What and Where components of the episodic memory in CA3 to a more efficient combination to act as a recall cue back to the entorhinal cortex and thereby neocortex (Treves and Rolls 1994, Rolls 2023, Rolls and Treves 2024). The firing rates of the CA1 neurons produced by the forward inputs from CA3 are produced as described above for the neocortex with Eqs. 2 and 3. Then the synapses between the active inputs and the high firing rate CA1 neurons are associatively modified by the Hebb associative learning rule Eq. 1. In the competitive network, the length of the synaptic weight vector on each neuron is then normalized to a length of 1, so that the different neurons compete on an equal basis (Rolls 2023). Also during training, the backprojections from CA1 to EntoWhat and EntoWhere are modified by Hebbian associative learning as shown in Eq. 1 to allow later recall when CA1 is active.

During recall, the connections from CA3 to CA1 operate in CA1 as usual in a competitive network to activate the correct neurons in CA1 via

the modified synapses (Rolls 2023) in a similar way to that described in Section 1.1 and Eqs. 2 and 3, with the sparseness being set during recall in CA1 in the same way as described above.

1.4 Rate model: CA3

The CA3 neurons are implemented as an attractor network (Treves and Rolls 1994, Rolls 2023, Rolls and Treves 2024). During training, the strong mossy fibre non-associatively modifiable synapses from the dentate granule cells with their very highly diluted connectivity (Fig. 1) select a new set of CA3 cells to be active for that episodic memory (Treves and Rolls 1992). The CA3 to CA3 associatively modifiable synapses for the attractor network then learn according to the Hebb rule Eq. 1, increasing the connection weights that are between the random new set of neurons currently firing because of the dentate input. To provide for recall, the synapses from the entorhinal cortex neurons that are active onto the currently active CA3 neurons are associatively modified according to Eq. 1, to set up the pathway that will later be used to trigger completion and recall in the CA3-CA3 attractor network (Treves and Rolls 1992). We identified the dentate to CA3 pathway as the pathway for recall of CA3 firing which is then completed by the CA3-CA3 attractor network connections because the entorhinal input has a relatively high number of synapses on each CA3 neuron (Fig. 1), and is associatively modifiable (Treves and Rolls 1992).

During recall, the entorhinal inputs to CA3 neurons trigger recall through the associatively modifiable synapses (Eq. 2). The CA3-CA3 connections then operate as an attractor network to complete what is likely to be an incomplete input, from e.g. EntoWhat only, not from EntoWhere, using Eq. 2. Care is taken to scale the activations to be stronger from CA3-CA3 than from the entorhinal cortex to CA3, to ensure that the completion performed by the CA3-CA3 network is fully evident in the active CA3 neurons. During this process, the activations are converted into rates according to Eq. 3, and the sparseness of the firing is controlled as described above. During recall, it is assumed that the dentate inputs do not make a major contribution to dominate the firing of the CA3 cells (Treves and Rolls 1992), with for example low acetylcholine during recall increasing the efficacy of the CA3-CA3 recurrent collaterals, as well as decreasing the learning rate in these synapses (Hasselmo and Bower 1993, Hasselmo, Schnell and Barkai 1995, Hasselmo, Wyble and Wallenstein 1996, Hasselmo 1999). (In contrast, during learning, high acetylcholine, perhaps triggered by reward or punishment inputs to the orbitofrontal cortex which in turn has connectivity to cholinergic neurons (Rolls, Deco, Huang and Feng 2022, Rolls 2022), may increase the synaptic learning rate in the CA3-CA3 connections, and decrease the efficacy of the recurrent collaterals in order to minimise effects of information already stored in CA3 (Hasselmo and Bower 1993, Hasselmo et al. 1995, Hasselmo

et al. 1996, Hasselmo 1999, Rolls and Treves 2024).)

2 Integrate-and-fire simulations of the hippocampal system

2.1 Implementation of the integrate-and-fire model of the hippocampal system with neuronal and synaptic dynamics

We use the mathematical formulation of the integrate-and-fire neurons and synaptic currents described by Brunel and Wang (2001). Here we provide a brief summary of this framework.

The dynamics of the sub-threshold membrane potential V of a neuron are given by the equation:

$$C_m \frac{dV(t)}{dt} = -g_m(V(t) - V_L) - I_{syn}(t), \tag{4}$$

Both excitatory and inhibitory neurons have a resting potential $V_L = -70mV$, a firing threshold $V_{thr} = -50mV$ and a reset potential $V_{reset} = -55mV$. The membrane parameters are different for both types of neurons: Excitatory (Inhibitory) neurons are modeled with a membrane capacitance $C_m = 0.5nF$ $(0.2nF)$, a leak conductance $g_m = 25nS$ $(20nS)$, a membrane time constant $\tau_m = 20ms$ $(10ms)$, and a refractory period $t_{ref} = 2ms$ $(1ms)$. Values are extracted from McCormick, Connors, Lighthall and Prince (1985).

When the threshold membrane potential V_{thr} is reached, the neuron is set to the reset potential V_{reset} at which it is kept for a refractory period τ_{ref} and the action potential is propagated to the other neurons.

Each network has $N_E = 5000$ excitatory neurons and $N_I = 1250$ inhibitory neurons which are conneced to each other, consistent with the observed proportions of the pyramidal neurons and interneurons in the cerebral cortex (Braitenberg and Schütz 1991, Abeles 1991). The synaptic current impinging on each neuron is given by the sum of recurrent excitatory currents ($I_{AMPA,rec}$ and $I_{NMDA,rec}$), the external excitatory current($I_{AMPA,ext}$), and the inhibitory current (I_{GABA}):

$$I_{syn}(t) = I_{AMPA,ext}(t) + I_{AMPA,rec}(t) + I_{NMDA,rec}(t) + I_{GABA}(t). \tag{5}$$

The recurrent excitation is mediated by the AMPA and NMDA receptors, inhibition by GABA receptors. In addition, the neurons are exposed to external Poisson input spike trains mediated by AMPA receptors at a rate of 2.4 kHz. These can be viewed as originating from $N_{ext} = 800$ external neurons at an average rate of 3 Hz per neuron, consistent with the spontaneous activity observed in the cerebral cortex (Wilson, O'Scalaidhe and Goldman-Rakic 1994, Rolls and Treves 1998). The currents are defined by:

$$I_{AMPA,ext}(t) = g_{AMPA,ext}(V(t)-V_E)\sum_{j=1}^{N_{ext}} s_j^{AMPA,ext}(t) \quad (6)$$

$$I_{AMPA,rec}(t) = g_{AMPA,rec}(V(t)-V_E)\sum_{j=1}^{N_E} w_{ji}^{AMPA} s_j^{AMPA,rec}(t) \quad (7)$$

$$I_{NMDA,rec}(t) = \frac{g_{NMDA}(V(t)-V_E)}{1+[Mg^{++}]exp(-0.062V(t))/3.57} \times \sum_{j=1}^{N_E} w_{ji}^{NMDA} s_j^{NMDA}(t) \quad (8)$$

$$I_{GABA}(t) = g_{GABA}(V(t)-V_I)\sum_{j=1}^{N_I} w_{ji}^{GABA} s_j^{GABA}(t) \quad (9)$$

where $V_E = 0$ mV, $V_I = -70$ mV, w_{ji} are the synaptic weights, s_j's the fractions of open channels for the different receptors and g's the synaptic conductances for the different channels. The NMDA synaptic current depends on the membrane potential and the extracellular concentration of Magnesium ($[Mg^{++}] = 1$ mM (Jahr and Stevens 1990)). The values for the synaptic conductances for excitatory neurons are $g_{AMPA,ext} = 2.08$ nS, $g_{AMPA,rec} = 0.104$ nS, $g_{NMDA} = 0.327$ nS and $g_{GABA} = 1,25$ nS ; and for inhibitory neurons $g_{AMPA,ext} = 1.62$ nS, $g_{AMPA,rec} = 0.081$ nS, $g_{NMDA} = 0.258$ nS and $g_{GABA} = 0.973$ nS for 800 synapses per neuron. These values are obtained from the ones used by Brunel and Wang (2001). The conductances and synaptic weights were set so that in an unstructured network the excitatory neurons have a spontaneous spiking rate of 3 Hz and the inhibitory neurons a spontaneous rate of 9 Hz. The fractions of open channels are described by:

$$\frac{ds_j^{AMPA,ext}(t)}{dt} = -\frac{s_j^{AMPA,ext}(t)}{\tau_{AMPA}} + \sum_k \delta(t-t_j^k) \quad (10)$$

$$\frac{ds_j^{AMPA,rec}(t)}{dt} = -\frac{s_j^{AMPA,rec}(t)}{\tau_{AMPA}} + \sum_k \delta(t-t_j^k) \quad (11)$$

$$\frac{ds_j^{NMDA}(t)}{dt} = -\frac{s_j^{NMDA}(t)}{\tau_{NMDA,decay}} + \alpha x_j(t)(1-s_j^{NMDA}(t)) \quad (12)$$

$$\frac{dx_j(t)}{dt} = -\frac{x_j(t)}{\tau_{NMDA,rise}} + \sum_k \delta(t-t_j^k) \quad (13)$$

$$\frac{ds_j^{GABA}(t)}{dt} = -\frac{s_j^{GABA}(t)}{\tau_{GABA}} + \sum_k \delta(t-t_j^k), \quad (14)$$

where $\tau_{NMDA,decay} = 100$ ms is the decay time for NMDA synapses, $\tau_{AMPA} = 6$ ms for AMPA synapses to allow for propagation effects (Hestrin,

Sah and Nicoll 1990, Spruston, Jonas and Sakmann 1995) and τ_{GABA} = 10 ms for GABA synapses (Salin and Prince 1996, Xiang, Huguenard and Prince 1998); $\tau_{NMDA,rise} = 2$ ms is the rise time for NMDA synapses (the rise times for AMPA and GABA are neglected because they are typically very short) and $\alpha = 0.5$ ms^{-1}. The sums over k represent a sum over spikes formulated as δ-Peaks $\delta(t)$ emitted by presynaptic neuron j at time t_j^k.

The equations were integrated numerically using a forward Euler method with step size 0.1 ms.

2.2 Connectivity

The architecture implemented with integrate-and-fire neurons is that shown in Fig. 1 (Rolls, Zhang and Feng 2024).

Each of the seven modules has full connectivity between the 5000 excitatory neurons and 1250 inhibitory neurons, i.e. w_{EtoI}, w_{ItoE} and w_{ItoI}. In an integrate-and-fire network, it is necessary to specify the connectivity strengths for the excitatory and the inhibitory neurons within each module. In the model attractor network (Brunel and Wang 2001, Rolls 2023), the default value for the excitatory to inhibitory (E to I) neuron connectivity, and for the inhibitory to excitatory connectivity, is 1.0. That value was used in the integrate-and-fire simulations described here except as follows. It was found that increasing the E to I connectivity to e.g. 9 could help to stabilize the whole network, and was especially important in CA3 and CA1. The actual values used for the E to I connectivity when not 1.0 were: EntoWhat=EntoWhere = 15; CA3 = 9; CA1 = 7. The only module where there was connectivity between the excitatory neurons within a module was CA3, where the value was increased between the 250 neurons used to store any one episodic memory to a value sufficient to maintain the attractor. The inhibitory neurons within a module inhibited each other with a connection weight of 1 (Brunel and Wang 2001).

All synaptic weight matrices were imported from the rate simulation described in the Methods of the main text, section *Rate Model of the neocortical-hippocampal system*, and were scaled to produce the minimal values to produce the effects illustrated in the figures in the main text. For the diluted connectivity between modules, the connectivity to each neuron was set up from a randomly permuted subset of neurons in the sending module, to ensure that no neuron had more than one connection from a sending neuron, as that can affect the memory capacity (Rolls 2012).

2.3 Calcium-dependent spike frequency adaptation mechanism

A specific implementation of the spike-frequency adaptation mechanism using Ca^{++}-activated K^+ hyper-polarizing currents (Liu and Wang 2001) is

described next, and was used by Deco and Rolls (2005). We assume that the intrinsic gating of K^+ After-Hyper-Polarizing current (I_{AHP}) is fast, and therefore its slow activation is due to the kinetics of the cytoplasmic Ca^{2+} concentration. This can be introduced in the model by adding an extra current term in the integrate-and-fire model, i.e. by adding I_{AHP} on the right hand of equation 15, which describes the evolution of the subthreshold membrane potential $V(t)$ of each neuron:

$$C_m \frac{dV(t)}{dt} = -g_m(V(t) - V_L) - I_{\text{syn}}(t) \tag{15}$$

where $I_{\text{syn}}(t)$ is the total synaptic current flow into the cell, V_L is the resting potential, C_{m} is the membrane capacitance, and g_{m} is the membrane conductance. The extra current term that is introduced into this equation is as follows:

$$I_{\text{AHP}} = -g_{\text{AHP}}[\text{Ca}^{2+}](V(t) - V_K) \tag{16}$$

where V_K is the reversal potential of the potassium channel. Further, each action potential generates a small amount (α) of calcium influx, so that I_{AHP} is incremented accordingly. Between spikes the $[\text{Ca}^{2+}]$ dynamics is modelled as a leaky integrator with a decay constant τ_{Ca}. Hence, the calcium dynamics can be described by the following system of equations:

$$\frac{d[\text{Ca}^{2+}]}{dt} = -\frac{[\text{Ca}^{2+}]}{\tau_{\text{Ca}}} \tag{17}$$

If $V(t) = \theta$, then $[\text{Ca}^{2+}] = [\text{Ca}^{2+}] + \alpha$ and $V = V_{\text{reset}}$, and these are coupled to the equations of the neural dynamics provided here and elsewhere (Rolls and Deco 2010). The $[\text{Ca}^{2+}]$ is initially set to be 0 μM, $\tau_{\text{Ca}} = 600$ ms, $\alpha = 0.002$, and $V_K = -80$ mV. As described in the main text, the g_{AHP} for all excitatory neurons was set to 150 nS, except for the entorhinal cortex where it was 450 nS, and in CA3 where it was set to 0 nS to help promote continuing firing. These values do produce marked adaptation, and were chosen so that the adaptation would be clearly evident in the Figures in the main text, and to emphasize what we propose is a key mechanism for maintaining cortical stability and minimizing runaway excitation between the excitatory neurons of the cortex.

2.4 Presynaptic adaptation or depression

Synaptic efficacy is modulated by the amount of available resources (x, normalized so that $0 < x < 1$) and the utilization parameter (u) that defines the fraction of resources used by each spike, reflecting the residual calcium level. When a spike occurs, an amount ux of the available resources is used to produce the postsynaptic current, thus reducing x. This process mimics

neurotransmitter depletion. Between spikes, x recovers to its baseline level ($x = 1$) with time constant τ_D (depressing). This phenomenological model reproduces the presynaptic adaptation or depression of cortical synapses (Mongillo, Barak and Tsodyks 2008). This was implemented as follows.

Each excitatory synapse to any excitatory neuron is modulated by the presynaptic adaptation factor $x_j(t)$ described by the following dynamics (Mongillo et al. 2008):

$$\frac{x_j(t)}{dt} = \frac{1 - x_j(t)}{\tau_D} - u x_j(t)) \sum_k \delta(t - t_j^k),$$

where $u = 0 - 1$ and $\tau_D = 500$ ms, and t_j^k is the time of the corresponding presynaptic spikes. For this work, a value of $u = 1$ was found suitable to help control the firing rates of the excitatory neurons in the coupled systems investigated in the neocortex and entorhinal cortex, and was 0.08 for CA3 and 0.1 for CA1 to help these neurons maintain their firing for several hundred ms.

2.5 The model parameters used in the integrate-and-fire simulations

The fixed parameters of the model are shown in Table 1, and not only provide information about the values of the parameters used in the simulations, but also enable them to be compared to experimentally measured values. The conductance values are similar to those in previous research on attractor networks (Brunel and Wang 2001, Rolls, Grabenhorst and Deco 2010, Rolls and Deco 2015), and the synaptic weights are scaled to produce similar currents from different sources such as excitatory to inhibitory, inhibitory to excitatory, and excitatory to excitatory, as in this previous research.

Table 1: Parameters used in the integrate-and-fire simulations

N_{E}	5000 in each module
N_{I}	1250 in each module
w_{EtoI}	1.0 default, except where stated
w_{ItoE}	1.0
w_{ItoI}	1.0
N_{ext}	800
ν_{ext}	2.4 kHz
C_{m} (excitatory)	0.5 nF
C_{m} (inhibitory)	0.2 nF
g_{m} (excitatory)	25 nS
g_{m} (inhibitory)	20 nS
V_{L}	–70 mV
V_{thr}	–50 mV
V_{reset}	–55 mV
V_{E}	0 mV
V_{I}	–70 mV
$g_{\mathrm{AMPA,ext}}$ (excitatory)	2.08 nS
$g_{\mathrm{AMPA,rec}}$ (excitatory)	0.104 nS
g_{NMDA} (excitatory)	0.327 nS
g_{GABA} (excitatory)	1.25 nS
$g_{\mathrm{AMPA,ext}}$ (inhibitory)	1.62 nS
$g_{\mathrm{AMPA,rec}}$ (inhibitory)	0.081 nS
g_{NMDA} (inhibitory)	0.258 nS
g_{GABA} (inhibitory)	0.973 nS
$\tau_{\mathrm{NMDA,decay}}$	100 ms
$\tau_{\mathrm{NMDA,rise}}$	2 ms
τ_{AMPA}	6 ms
τ_{GABA}	10 ms
α	0.5 ms^{-1} for NMDA dynamics
τ_{D}	500 ms presynaptic depression time constant
u	0.08 - 1.0 presynaptic depression utilization factor, see values above

References

Abeles, A. (1991). *Corticonics*, Cambridge University Press, New York.

Braitenberg, V. and Schütz, A. (1991). *Anatomy of the Cortex*, Springer Verlag, Berlin.

Brunel, N. and Wang, X. J. (2001). Effects of neuromodulation in a cortical network model of object working memory dominated by recurrent inhibition, *Journal of Computational Neuroscience* **11**: 63–85.

Deco, G. and Rolls, E. T. (2005). Sequential memory: a putative neural and synaptic dynamical mechanism, *Journal of Cognitive Neuroscience* **17**: 294–307.

Hasselmo, M. E. (1999). Neuromodulation: acetylcholine and memory consolidation, *Trends Cogn Sci* **3**: 351–359.

Hasselmo, M. E. and Bower, J. M. (1993). Acetylcholine and memory, *Trends in Neurosciences* **16**: 218–222.

Hasselmo, M. E., Schnell, E. and Barkai, E. (1995). Dynamics of learning and recall at excitatory recurrent synapses and cholinergic modulation in rat hippocampal region ca3, *J Neurosci* **15**: 5249–62.

Hasselmo, M. E., Wyble, B. P. and Wallenstein, G. V. (1996). Encoding and retrieval of episodic memories: role of cholinergic and gabaergic modulation in the hippocampus, *Hippocampus* **6**: 693–708.

Hestrin, S., Sah, P. and Nicoll, R. (1990). Mechanisms generating the time course of dual component excitatory synaptic currents recorded in hippocampal slices, *Neuron* **5**: 247–253.

Jahr, C. and Stevens, C. (1990). Voltage dependence of NMDA-activated macroscopic conductances predicted by single-channel kinetics, *Journal of Neuroscience* **10**: 3178–3182.

Liu, Y. and Wang, X.-J. (2001). Spike-frequency adaptation of a generalized leaky integrate-and-fire model neuron, *Journal of Computational Neuroscience* **10**: 25–45.

McCormick, D., Connors, B., Lighthall, J. and Prince, D. (1985). Comparative electrophysiology of pyramidal and sparsely spiny stellate neurons in the neocortex, *Journal of Neurophysiology* **54**: 782–806.

Mongillo, G., Barak, O. and Tsodyks, M. (2008). Synaptic theory of working memory, *Science* **319**: 1543–6.

Rolls, E. T. (1995). A model of the operation of the hippocampus and entorhinal cortex in memory, *International Journal of Neural Systems* **6**: 51–70.

Rolls, E. T. (2012). Advantages of dilution in the connectivity of attractor networks in the brain, *Biologically Inspired Cognitive Architectures* **1**: 44–54.

Rolls, E. T. (2022). The hippocampus, ventromedial prefrontal cortex, and episodic and semantic memory, *Prog Neurobiol* **217**: 102334.

Rolls, E. T. (2023). *Brain Computations and Connectivity*, Oxford University Press, Open Access, Oxford.

Rolls, E. T. and Deco, G. (2010). *The Noisy Brain: Stochastic Dynamics as a Principle of Brain Function*, Oxford University Press, Oxford.

Rolls, E. T. and Deco, G. (2015). Stochastic cortical neurodynamics underlying the memory and cognitive changes in aging, *Neurobiol Learn Mem* **118**: 150–61.

Rolls, E. T. and Treves, A. (1998). *Neural Networks and Brain Function*, Oxford University Press, Oxford.

Rolls, E. T. and Treves, A. (2024). A theory of hippocampal function: New developments, *Prog Neurobiol* **238**: 102636.

Rolls, E. T., Grabenhorst, F. and Deco, G. (2010). Choice, difficulty, and confidence in the brain, *Neuroimage* **53**: 694–706.

Rolls, E. T., Deco, G., Huang, C. C. and Feng, J. (2022). The human orbitofrontal cortex, vmpfc, and anterior cingulate cortex effective connectome: emotion, memory, and action, *Cereb Cortex* **33**: 330–356.

Rolls, E. T., Zhang, C. and Feng, J. (2024). Hippocampal storage and recall of neocortical 'what' - 'where' representations, *Hippocampus* p. doi: 10.1002/hipo.23636.

Salin, P. and Prince, D. (1996). Spontaneous GABA-A receptor mediated inhibitory currents in adult rat somatosensory cortex, *Journal of Neurophysiology* **75**: 1573–1588.

Spruston, N., Jonas, P. and Sakmann, B. (1995). Dendritic glutamate receptor channel in rat hippocampal CA3 and CA1 pyramidal neurons, *Journal of Physiology* **482**: 325–352.

Treves, A. and Rolls, E. T. (1992). Computational constraints suggest the need for two distinct input systems to the hippocampal ca3 network, *Hippocampus* **2**: 189–99.

Treves, A. and Rolls, E. T. (1994). A computational analysis of the role of the hippocampus in memory, *Hippocampus* **4**: 374–391.

Wilson, F. A. W., O'Scalaidhe, S. P. and Goldman-Rakic, P. (1994). Functional synergism between putative gamma-aminobutyrate-containing neurons and pyramidal neurons in prefrontal cortex, *Proceedings of the National Academy of Science* **91**: 4009–4013.

Xiang, Z., Huguenard, J. and Prince, D. (1998). GABA-A receptor mediated currents in interneurons and pyramidal cells of rat visual cortex, *Journal of Physiology* **506**: 715–730.